

AWARD NUMBER: W81XWH-14-1-0329

TITLE: Inhibition of Retinoblastoma Protein Inactivation

PRINCIPAL INVESTIGATOR: Seth M. Rubin, Ph.D.

CONTRACTING ORGANIZATION: University of California, Santa Cruz
Santa Cruz, CA 95064

REPORT DATE: November 2017

TYPE OF REPORT: Final

PREPARED FOR: U.S. Army Medical Research and Materiel Command
Fort Detrick, Maryland 21702-5012

DISTRIBUTION STATEMENT: Approved for Public Release;
Distribution Unlimited

The views, opinions and/or findings contained in this report are those of the author(s) and should not be construed as an official Department of the Army position, policy or decision unless so designated by other documentation.

REPORT DOCUMENTATION PAGEForm Approved
OMB No. 0704-0188

Public reporting burden for this collection of information is estimated to average 1 hour per response, including the time for reviewing instructions, searching existing data sources, gathering and maintaining the data needed, and completing and reviewing this collection of information. Send comments regarding this burden estimate or any other aspect of this collection of information, including suggestions for reducing this burden to Department of Defense, Washington Headquarters Services, Directorate for Information Operations and Reports (0704-0188), 1215 Jefferson Davis Highway, Suite 1204, Arlington, VA 22202-4302. Respondents should be aware that notwithstanding any other provision of law, no person shall be subject to any penalty for failing to comply with a collection of information if it does not display a currently valid OMB control number. **PLEASE DO NOT RETURN YOUR FORM TO THE ABOVE ADDRESS.**

1. REPORT DATE November 2017		2. REPORT TYPE Final		3. DATES COVERED 1 Sep 2014 - 31 Aug 2017	
4. TITLE AND SUBTITLE Inhibition of Retinoblastoma Protein Inactivation				5a. CONTRACT NUMBER	
				5b. GRANT NUMBER W81XWH-14-1-0329	
				5c. PROGRAM ELEMENT NUMBER	
6. AUTHOR(S) Seth M. Rubin, Ph.D. E-mail: srubin@ucsc.edu				5d. PROJECT NUMBER	
				5e. TASK NUMBER	
				5f. WORK UNIT NUMBER	
7. PERFORMING ORGANIZATION NAME(S) AND ADDRESS(ES) University of California, Santa Cruz 1156 High St. Santa Cruz, CA 95064				8. PERFORMING ORGANIZATION REPORT NUMBER	
9. SPONSORING / MONITORING AGENCY NAME(S) AND ADDRESS(ES) U.S. Army Medical Research and Materiel Command Fort Detrick, Maryland 21702-5012				10. SPONSOR/MONITOR'S ACRONYM(S)	
				11. SPONSOR/MONITOR'S REPORT NUMBER(S)	
12. DISTRIBUTION / AVAILABILITY STATEMENT Approved for Public Release; Distribution Unlimited					
13. SUPPLEMENTARY NOTES					
14. ABSTRACT The objective of this project is to discover and characterize molecules that inhibit breast cancer cell proliferation by maintaining activity of the retinoblastoma protein (Rb). Rb is inactivated to drive proliferation in normal and cancer cells by phosphorylation, which dissociates the E2F transcription factor from Rb to activate S phase genes. Our goal is to find and characterize molecules that stabilize the complex between phosphorylated Rb and E2F. During the project period, we tested our proposed mechanism for how molecules may enhance the affinity of phosphorylated Rb (phosRb) for E2F by disrupting the compact phosRb conformation. We identified a proof-of-concept peptide that increases phosRb-affinity, we developed a fluorescence-based assay to identify small molecule enhancers of phos-Rb affinity, we performed a high throughput screen and further tested hits in the primary screen, and we began pursuing additional fragment-based approaches to identifying lead compounds.					
15. SUBJECT TERMS cell cycle, Retinoblastoma protein, E2F transcription factor, high throughput screen, drug discovery, x-ray crystallography					
16. SECURITY CLASSIFICATION OF:			17. LIMITATION OF ABSTRACT	18. NUMBER OF PAGES	19a. NAME OF RESPONSIBLE PERSON USAMRMC
a. REPORT	b. ABSTRACT	c. THIS PAGE			19b. TELEPHONE NUMBER (include area code)
Unclassified	Unclassified	Unclassified	Unclassified	16	

Table of Contents

	<u>Page</u>
1. Introduction.....	4
2. Keywords.....	4
3. Accomplishments.....	4-9
4. Impact.....	9
5. Changes/Problems.....	9
6. Products.....	9
7. Participants & Other Collaborating Organizations.....	9-10
8. Special Reporting Requirements.....	10
9. Appendices.....	10-16

1.0 INTRODUCTION

The Rb pathway connects environmental and intracellular growth signals to the cell-cycle machinery that drives cell division. Inactivation of Rb pathway function is found in most human cancers, including breast cancer. Inhibition of cell proliferation by Rb is linked to its direct binding of E2F transcription factors and repression of E2F activity. Rb inactivation occurs upon Cdk phosphorylation, which induces E2F release and activation of S phase genes. *Our overarching hypothesis is that we can modulate Rb activity directly with small molecules that inhibit or stabilize its association with E2F and thus control breast cancer cell proliferation.* This project aimed to test this hypothesis with a proof-of-concept peptide, to identify such molecules with high-throughput screening, to validate hits in secondary and cellular assays, and to characterize the mechanism of lead compound interaction with Rb. In the last two years of the project period, we also developed a method to perform fragment based screening by x-ray crystallography.

2.0 KEYWORDS

Retinoblastoma (Rb) pathway, E2F transcription factor, cancer, cell-cycle inhibition, activation, modulation, inhibition, high throughput screening, fragment-based screening, x-ray crystallography.

3.0 ACCOMPLISHMENTS

Summary:

We successfully tested the hypothesis that molecules can be identified that enhance the affinity of phosphorylated Rb for E2F, and we developed a robust assay to identify small molecules that generate this desired effect. Our results in these experiments and the results of our pilot screen were published in ACS Chemical Biology during the project period. We performed experiments to validate the efficacy of compounds identified as hits in a large library screen (in collaboration with the Sanford Burnham Institute) in our primary screen, but we found that they do not robustly enhance Rb-E2F affinity, and we found no evidence that they bind Rb. We also laid the foundation for an additional approach to identifying lead compounds using fragment-based screening by x-ray crystallography.

Goals:

- 1) Test model for how compounds can enhance Rb-E2F affinity by disrupting the compact conformation of phosphorylated Rb.
- 2) Develop a high throughput, fluorescence based assay and screen a library of small molecules
- 3) Develop tools and protocols for fragment based screening

Detailed Accomplishments:

Task 1: Test hypothesis that disrupting phosphorylation-induced Rb conformational changes enhances

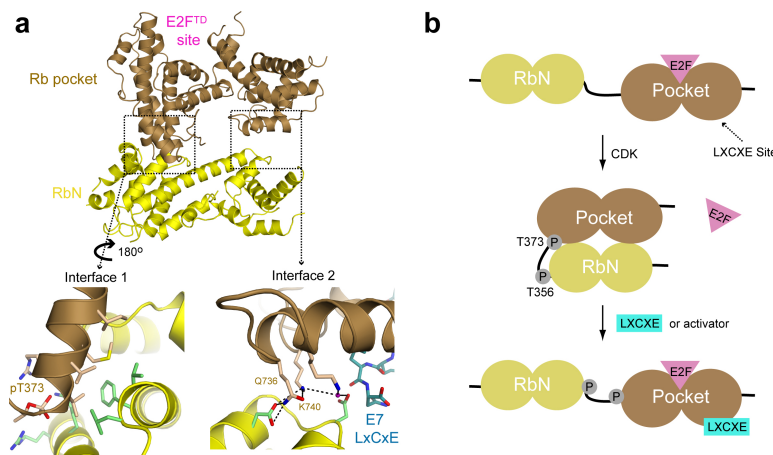


Figure 1. Model for activation of Rb. (a) Structure of phosphorylated Rb. Docking between the Rb N-terminal domain (RbN, yellow) and the pocket domain (brown) occurs across two interfaces. Interface 1 is mediated by T373 phosphorylation. Interface 2 is near the LxCxE-binding cleft in the pocket. The E7 peptide (cyan backbone), which is shown bound at its site in the unphosphorylated pocket, clashes with RbN residues at the interface. (b) Phosphorylation of sites in the Rb interdomain linker induces a conformational change that allosterically inhibits E2F binding. We find that an LxCxE peptide and a protein containing that sequence acts as an activator by binding Rb and inhibiting the RbN-pocket interdomain association.

E2F binding

Our goal to develop Rb activators is motivated by our discovery of the structural mechanism underlying how the Rb-E2F complex is inhibited by Rb phosphorylation (Figure 1). Our previous work demonstrated that T373 phosphorylation in Rb induces an interdomain association between the Rb N-terminal domain (RbN) and the so-called pocket domain, which allosterically opens the E2F binding cleft in the pocket to weaken affinity. RbN-pocket association occurs across two interfaces (Figure 1a), both of which must be formed to open up the E2F-binding site and disrupt interactions between the pocket and E2F. The RbN position at one interface is close to the “LxCxE binding” site in the pocket domain. This cleft is a well characterized binding site for viral and cellular proteins that contain an LxCxE amino acid sequence. From a structural alignment (Figure 1a), the binding of the LxCxE peptide and interdomain docking appear incompatible. We reasoned that molecules that inhibit interdomain docking would stabilize E2F binding to phosphorylated Rb by preventing the allosteric opening of the E2F binding site (Figure 1b). Moreover, because the LxCxE peptide binds near the second RbN-pocket interface (Interface 2 in Figure 1a), we hypothesized that it would disrupt docking and act as an activator. In the proposal period, we tested the effects of the LxCxE peptide from the HPV E7 protein on E2F binding to Rb using a fluorescence polarization (FP) assay (Figure 2). The affinity of E2F for unphosphorylated Rb ($K_d = 4.3 \pm 0.2$ nM) is 8-fold tighter than its affinity for phosphorylated Rb in this assay ($K_d = 31 \pm 4$ nM). In the presence of 10 μ M E7 LxCxE peptide, phosphorylated Rb binds E2F with 2-fold higher affinity ($K_d = 16 \pm 2$ nM), which implicates the LxCxE peptide as an example of a desired Rb activator molecule. In the presence of 2 μ M full length E7 protein, E2F binds phosphorylated Rb with similar affinity ($K_d = 4.6 \pm 0.3$ nM) as unphosphorylated Rb.

We found that the LxCxE peptide and full-length E7 increased RbNP-E2F affinity with $EC_{50} = 190 \pm 40$ nM and $EC_{50} = 10 \pm 2$ nM respectively (Figure 2b). The greater potency of the full-length protein correlates with its known 20-fold greater affinity for the Rb pocket domain. We suggest that the greater highest activity of the protein (~100%) compared to the peptide (~70%) may result from the fact that its larger size is better suited for occluding the RbN-pocket interface. We found that the LxCxE-peptide and E7 protein do not affect E2F binding to Rb if the docking interface is mutated (Q736A/K740A), which supports further our proposal that these activators function by disrupting interdomain docking. We also tested two LxCxE-like peptides from

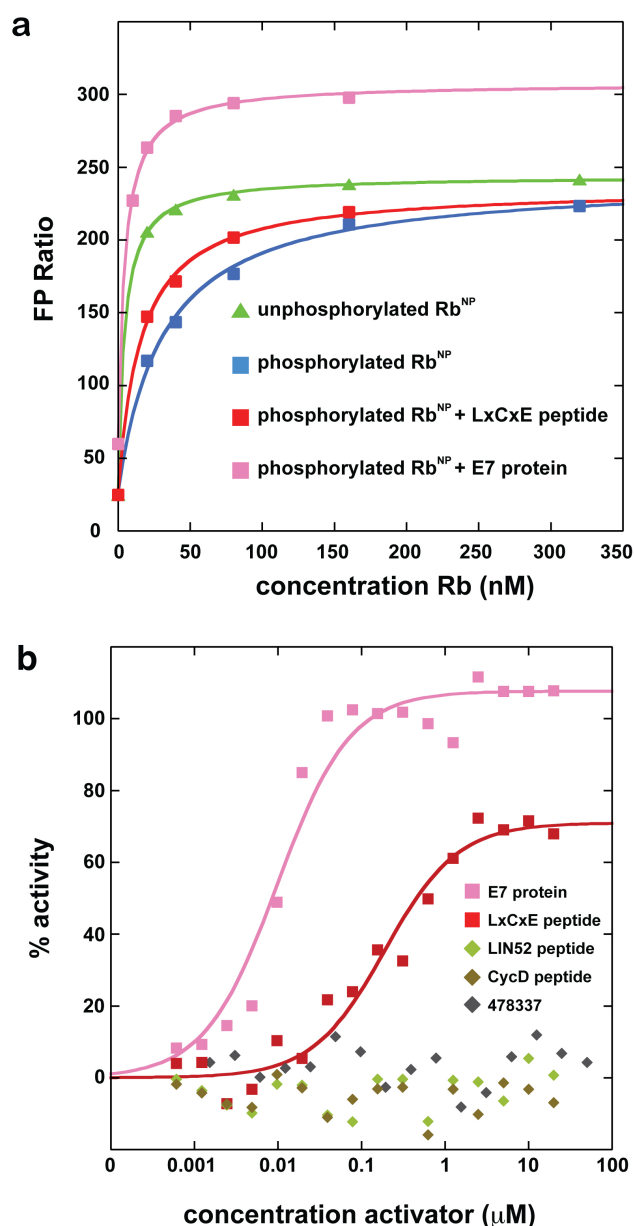


Figure 2. LxCxE peptide acts as an Rb activator. (a) Titration of unphosphorylated and phosphorylated Rb into E2F. In the presence of the E7 LxCxE peptide and full-length E7 protein (pink), the affinity is increased. (b) EC_{50} measurement of LxCxE peptide and E7 protein activity. Compound #478337 and LxCxE variant peptides from Cyclin D and LIN52 do not show activity.

Cyclin D (no hydrophobic in +2 position) and LIN52 (LxSxE), which have weak affinity for Rb. These variant peptides and a compound previously reported to bind the LxCxE cleft (compound #478337 show no effect in the Rb activation assay (Figure 2b). These results were published along with detailed methods in our ACS Chemical Biology paper (attached as appendix).

Task 2: Perform high throughput screen for small molecule enhancers of Rb-E2F affinity

Subtask 2.1: Optimize fluorescence polarisation assay for 1536-well format

We originally developed a fluorescence polarization (FP) assay for 384-well plates (included as preliminary data in proposal application) that required testing and potential optimization for the 1536-well higher-throughput format. The assay comprises a peptide corresponding to the E2F transactivation domain (human E2F2 amino acids 409-428) synthesized with a tetramethylrhodamine dye (TMR) at its N-terminus (E2F^{TMR}). This peptide is incubated with a recombinant Rb^{NP} construct with or without compounds. Phosphorylation of this Rb construct recapitulates the loss of E2F^{TD} binding, which is necessary and sufficient for Rb inactivation in cells.

In the smaller-well format, we recapitulated the binding pharmacology of the assay FP signal (mP) with respect to E2F^{TMR}, where equivalence (signal plateau) was obtained at ~12.5 nM consistent with a 1:1 E2F^{TMR}: Rb^{NP} complex (Figure 3, top left). They also recapitulated the reduction of binding upon phosphorylation of Rb^{NP} (□) to phosRb^P (□) and increase of binding with the positive LxCxE (□) peptide control, which restores Rb^{NP} to tight binding (Figure 3, top right). Additionally, the signal was stable up to 3 hr and the assay was very tolerant up to 4% DMSO (v/v) (Figure 3, bottom).

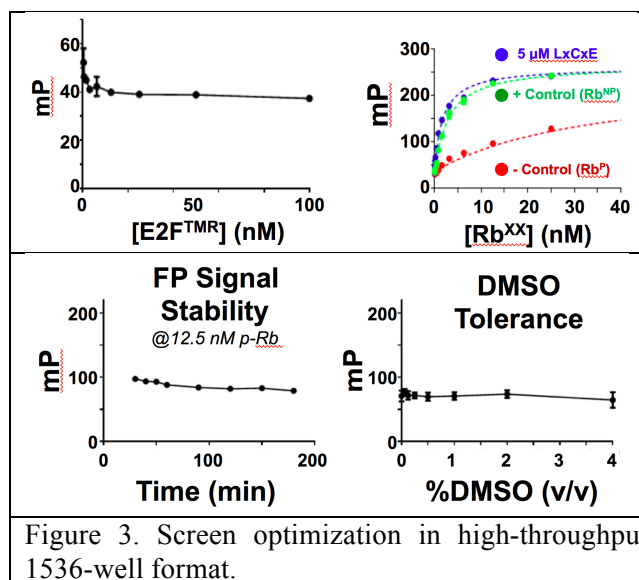
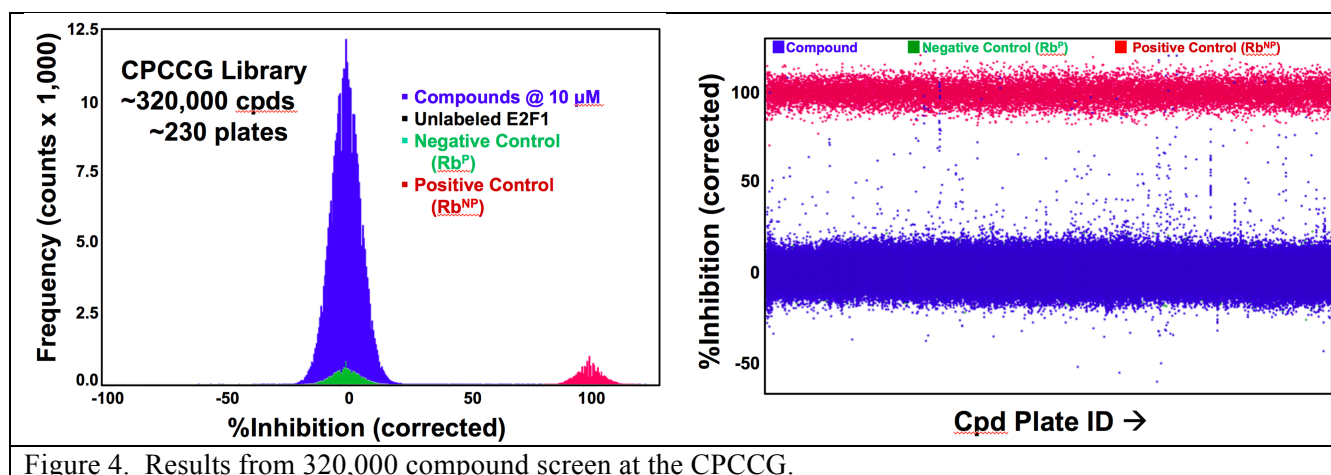


Figure 3. Screen optimization in high-throughput 1536-well format.

Subtask 2.2: Perform screen with compound library sets

Based on assay validation and implementation, we completed scale-up of a production lot of protein reagents (~100 μL of 100 μM E2F^{TMR}, ~50 μL of 80 μM Rb^{NP}, and 200 μL of phosphorylated Rb^{NP}). Reagents were generated in the Rubin laboratory, quality control was performed with an FP assay at UCSC, and the proteins were sent to the Sanford Burnham Conrad Prebys Center for Chemical Genomics (CPCCG). CPCCG completed the full HTS campaign on 5/15/15, testing 320,000 compounds. Assay performance during the HTS campaign was robust as shown in the Table above, with no individual plate running with less than 0.65 Z'. Based on the superior performance, we set the threshold at 30% inhibition as the hit rate. The hit rate at this threshold (0.07%) was low as expected for this difficult target class of a protein-protein interaction.

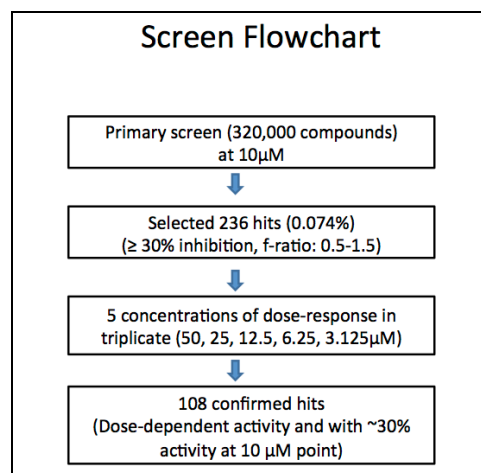
Parameter	Value
Positive Control (mP)	195.7 ± 8.6
Negative Control (mP)	52.6 ± 6.9
Signal to noise	17.10 ± 1.91
Z'	0.67 ± 0.03
Hits (>30% activity)	236
Hit Rate %	0.07



The frequency distribution and the scattergram for the screen (Figure 3) are consistent with a robust normally distributed centroid of zero activity, with clear hits. At the threshold of >30% activity, we selected 236 compounds, which had an F-ratio between 0.5 – 1.5 (an indication that the compound is not fluorescent or absorption artifact), as primary hits.

Subtask 2.3: Cherry-pick hits and rescreen with dose-response in triplicate

Because of the relatively low number of primary hits obtained, we forewent the process of triplicate cherry picking for a confirmation at the single original screening concentration, but rather went straightaway into triplicate 5-point dose-response analysis (50, 25, 12.5, 6.25, 3.125 μM final) using the CPCCG “direct dilution” paradigm with their Labcyte Echo 555 acoustic drop ejection technology, where every point on a dilution curve represents a true independent (rather than serial) dispensing event. With this, we confirmed 108 compounds as giving a dose-response curve with at least 30% inhibition at 10 μM . The flowchart of hit progression is shown on the right. Ultimately, 20 confirmed hits showed an estimated $\text{IC}_{50} < 10\mu\text{M}$.



Subtask 2.4: Filter hits with PANS and select compounds to move forward with validation.

CPCCG’s Cheminformatics team clustered the 108 confirmed hits by scaffold class, sorted them by potency, and also flagged PAINS (Pan Assay Interfering Compounds, which are common false positives). This analysis resulted in 18 scaffold groups (clusters containing 2 – 9 exemplars) and 38 singletons (only one exemplar in the group) to account for all 108 confirmed hits. We also called out the most potent exemplar of each cluster, though we deprioritized those compounds with dose response curves, which did not fit well. A few of the clusters showed a span of 5-fold potency, which suggested emergent SAR and provided confidence that these are bonafide tractable hits.

Subtask 2.5: Validate hits from primary screen and prepare reagents for a cyclic peptide library screen

Using the above analysis, the list of 108 confirmed hits was pared down to 40 top candidates. We next attempted to validate these hits by ordering fresh, dry compounds and testing them in the same FP assay. We found that about half of the 40 compounds did not repeat in the assay and the other half induced changes to the E2F FP signal even in the absence of Rb target. We conclude that these compounds are aggregating the E2F probe peptide and are not suitable lead compounds.

Based on these results, we decided not to pursue any hits from the initial small molecule library screen and instead focus on screening larger molecules that may be better suited for modulating protein-protein interactions. We successfully prepared the required protein to screen cyclic peptide libraries in collaboration with Professor Scott Lokey at UCSC.

Task 3: Crystallize Rb and E2F constructs for fragment based screening

As an additional approach to finding molecules that modulate Rb-E2F binding in the FP or similar assay, we created tools for a fragment-based approach to identify molecules that bind either Rb or E2F. Once we identify fragments that bind these proteins, we will synthetically build molecules that are potentially capable of modulating the complex affinity. We are taking an x-ray crystallography approach in which a small fragment library will be screened by soaking compounds into crystals of Rb or E2F. Following x-ray data collection, new electron density corresponding to the fragments will be observable if there is binding, and the structural data can be used to develop more potent binders. This approach requires crystal forms of Rb and E2F that diffract well and are highly reproducible. From past work, we have such a crystal form of the Rb pocket domain, and this past year we focused on producing a suitable crystal of E2F. We were able to successfully grow crystals of the E2F4 marked-box and coiled-coiled domains (Figure 3), which are the primary structured regions of the E2F transcription factor. These crystals diffract to 1.8 angstroms and we solved the structure of the E2F4 domain using molecular replacement.

We next took these crystals and soaked them with 50 different primary amine-containing molecular fragments in an in-house library. We chose to use amines because the reactive group will facilitate future chemistry. After soaking crystals with five fragments at a time, we collected x-ray diffraction data sets. Several of the crystals have new electron density near E2F4 that we propose is the bound fragment. An example is shown in Figure 5.

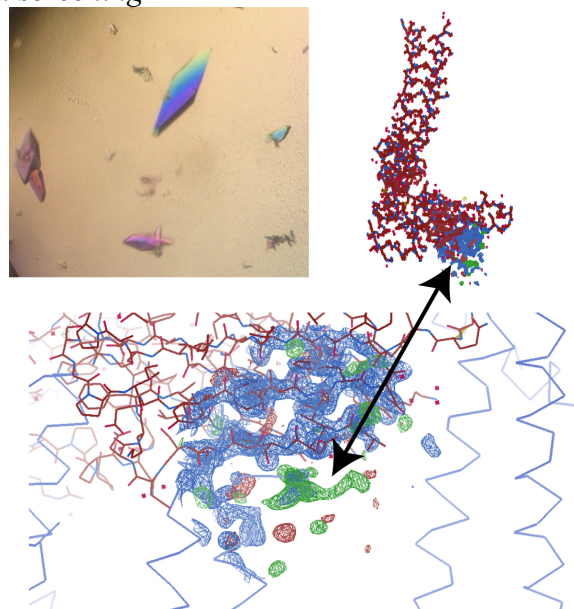


Figure 5. (Top, left) Crystals grown for E2F4 that diffract to 1.8 angstroms. (Top, right) Structure of E2F4 and electron density after soaking with small molecule amines. (Bottom) Close-up view of positive electron density (green) near the E2F4 molecule. This electron density likely corresponds to soaked fragment. The red chain is the E2F4 in the asymmetric unit, the blue chains are symmetry related E2F4 molecules in the crystal.

Training Opportunities: Nothing to report

Dissemination of Results:

Publication

Pye C.R., Bray W.M., Brown E.R., Burke J.R., Lokey R.S., Rubin S.M. A strategy for direct chemical activation of the retinoblastoma protein. ACS Chem Biol. 2016 May 20;11(5):1192-7.

Outreach

Presentation to Santa Cruz Cancer Benefit Group in downtown Santa Cruz, CA. ~60 attendees. July 22nd, 2017.

Future plans:

Nothing to report (final report).

4.0 IMPACT

Our research is having impact by establishing an innovative approach to breast cancer therapeutic development. Most approaches to date for preventing cancer cell cycle progression have focused on upstream Cdk inhibitors. This approach is traditional because enzyme active sites are easily blocked with small molecules. We are proposing a transformative approach that restores tumor suppressor function in the presence of upregulated inactivating kinases. The use of molecules to stimulate the gain of tumor suppressor function through direct interaction has been little explored, and our research therefore has the potential to demonstrate the therapeutic accessibility of a novel class of targets. In addition, our research will provide important insights into how therapeutics may function by manipulating protein-protein interactions, an increasingly important class of cancer targets. For breast cancer treatment in particular, the discovery of molecules that target Rb directly will be a breakthrough towards the development of safe and effective chemotherapeutics.

5.0 CHANGES / PROBLEMS

We encountered no technical problems. We did not find an ideal lead compound from our screen of the CPCCG small molecule collection, so we pursued some additional approaches outlined in our proposal and described above. The overall goals and aims remained the same throughout the project period, and there were no changes to protocols.

6.0 PRODUCTS

Publication

Pye C.R., Bray W.M., Brown E.R., Burke J.R., Lokey R.S., Rubin S.M. A strategy for direct chemical activation of the retinoblastoma protein. ACS Chem Biol. 2016 May 20;11(5):1192-7.

Patent

Rubin S.M., Burke J.R. Patent No. 9365621, A Method for Preventing Neoplastic Transformation by Inhibition of Retinoblastoma Protein Inactivation

7.0 PARTICIPANTS

Individuals in Rubin Laboratory working on project:

Name: Dr. Seth Rubin

Role: PI

Total Person Months: 6

Contribution to project: Oversee project, data interpretation, and communication of results

Funding support: 2 summer calendar months from grant. Other support from UCSC salary.

Name: Cameron Pye

Role: Graduate Student Researcher

Total Person Months: 3

Contribution to project: Fluorescence assay optimization and proof-of-concept experiments

Name: Caileen Brison

Role: Graduate Student Researcher

Total Person Months: 8

Contribution to project: Generation of reagents, screen hit follow-up experiments

Name: Tyler Liban

Role: Graduate Student Researcher

Total Person Months: 9

Contribution to project: Biophysical validation assays and preliminary crystallization of protein targets and fragment soaking

Changes in Key Personnel:

Nothing to Report

Partners:

Conrad Prebys Center for Chemical Genomics, Sanford Burnham Institute

San Diego, California

Facilities and Collaboration

8.0 SPECIAL REPORTING REQUIREMENTS

None

9.0 APPENDICES

Publication

Pye C.R., Bray W.M., Brown E.R., Burke J.R., Lokey R.S., Rubin S.M. A strategy for direct chemical activation of the retinoblastoma protein. ACS Chem Biol. 2016 May 20;11(5):1192-7.

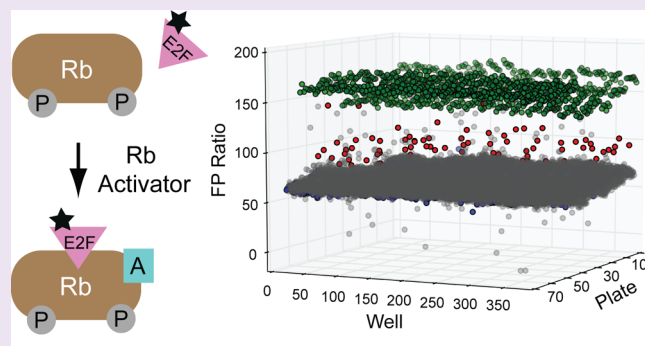
A Strategy for Direct Chemical Activation of the Retinoblastoma Protein

Cameron R. Pye, Walter M. Bray, Elise R. Brown, Jason R. Burke, R. Scott Lokey, and Seth M. Rubin*

Department of Chemistry and Biochemistry, University of California, Santa Cruz, California 95064, United States

S Supporting Information

ABSTRACT: The retinoblastoma (Rb) tumor suppressor protein negatively regulates cell proliferation by binding and inhibiting E2F transcription factors. Rb inactivation occurs in cancer cells upon cyclin-dependent kinase (Cdk) phosphorylation, which induces E2F release and activation of cell cycle genes. We present a strategy for activating phosphorylated Rb with molecules that bind Rb directly and enhance affinity for E2F. We developed a fluorescence polarization assay that can detect the effect of exogenous compounds on modulating affinity of Rb for the E2F transactivation domain. We found that a peptide capable of disrupting the compact inactive Rb conformation increases affinity of the repressive Rb–E2F complex. Our results demonstrate the feasibility of discovering novel molecules that target the cell cycle and proliferation through directly targeting Rb rather than upstream kinase activity.



Rb regulates proliferation through controlling the cell cycle, differentiation, senescence, and cell survival.^{1–4} Rb orchestrates proper cellular signals with the mechanics of cell cycle progression, and cancer cells almost invariably have alterations in Rb pathway components that enable uncontrolled cell proliferation.^{1,2,4–7} While deletion of the gene and full loss of the Rb protein is observed in some cancers, in the vast majority of cases, Rb pathway inactivation in cancer cells is achieved through activation of cyclin/Cdk complexes or inactivation of proteins that inhibit Cdk activity.^{2,5,7} Thus, chemotherapeutic strategies that directly promote Rb activity would be relevant to most tumors.

We describe here a novel approach to reversing Rb inactivation with molecules that directly bind Rb itself. There are potential therapeutic advantages to such compounds over current Cdk inhibitors, including potency and specificity.⁸ In addition, the specificity of such molecules would give them unprecedented advantages for studying the Rb pathway and its role in tumor suppression. For example, currently the only chemical approach to preventing Rb inactivation is through Cdk inhibition, which has off-target effects from preventing phosphorylation of other substrates.⁸ Despite these motivations, no direct chemical probes of Rb exist beyond molecules that specifically inhibit Rb association with viral oncoproteins.⁹

Rb arrests cells largely due to its ability to repress E2F-mediated gene expression.³ Rb binds E2F primarily through an association of its so-called “pocket” domain with the E2F transactivation domain (E2F^{TD}). E2F^{TD} binding by the pocket is necessary for Rb activity in growth suppression, cell cycle control, and E2F inhibition.³ The Rb pocket domain has an additional protein interaction cleft known as the “LxCxE” site, which binds oncogenic viral proteins and cellular proteins

containing the LxCxE ϕ sequence motif (ϕ is a hydrophobic residue).^{3,10} Several specific Cdk phosphorylation events inhibit E2F binding upon S phase entry,^{11,12} however Thr373 phosphorylation has the most pronounced effect in quantitative *in vitro* assays.^{13,14} Evidence also suggests that Thr373 phosphorylation is the most critical event for Rb inactivation *in vivo*. Thr373 is the only phosphorylation site sufficient for Cdk-induced inactivation of Rb in cells, and mutation of Thr373 significantly inhibits Cdk-induced Rb–E2F dissociation and E2F activation.^{15–17}

We set out to identify molecules that directly activate Rb by stabilizing the association of E2F^{TD} with Cdk-phosphorylated Rb. To search for such compounds, we crafted a fluorescence polarization assay that is amenable to high throughput screening. An E2F^{TD} peptide (human E2F2 amino acids 409–428) was synthesized with a tetramethylrhodamine dye (TMR) at its N-terminus (E2F^{TMR}). We assayed binding of E2F^{TMR} to an Rb protein construct (Rb^{NP}) that contains the Rb N-terminal domain (RbN) and pocket domain but lacks internal loops in each domain (residues 55–787, Δ 245–267, Δ 582–642).¹⁴ This minimized Rb construct contains two phosphorylation sites (T356 and T373) and the structural elements necessary and sufficient for recapitulating the inhibitory effect of T373 phosphorylation on E2F^{TD} binding.¹⁴

We assayed fluorescence polarization (FP) ratios in 384-well format using 10 nM E2F^{TMR} (Figure 1a). The FP ratio for free E2F^{TMR} is \sim 20 in our assay conditions, and the FP ratio

Received: January 6, 2016

Accepted: February 4, 2016

Published: February 4, 2016

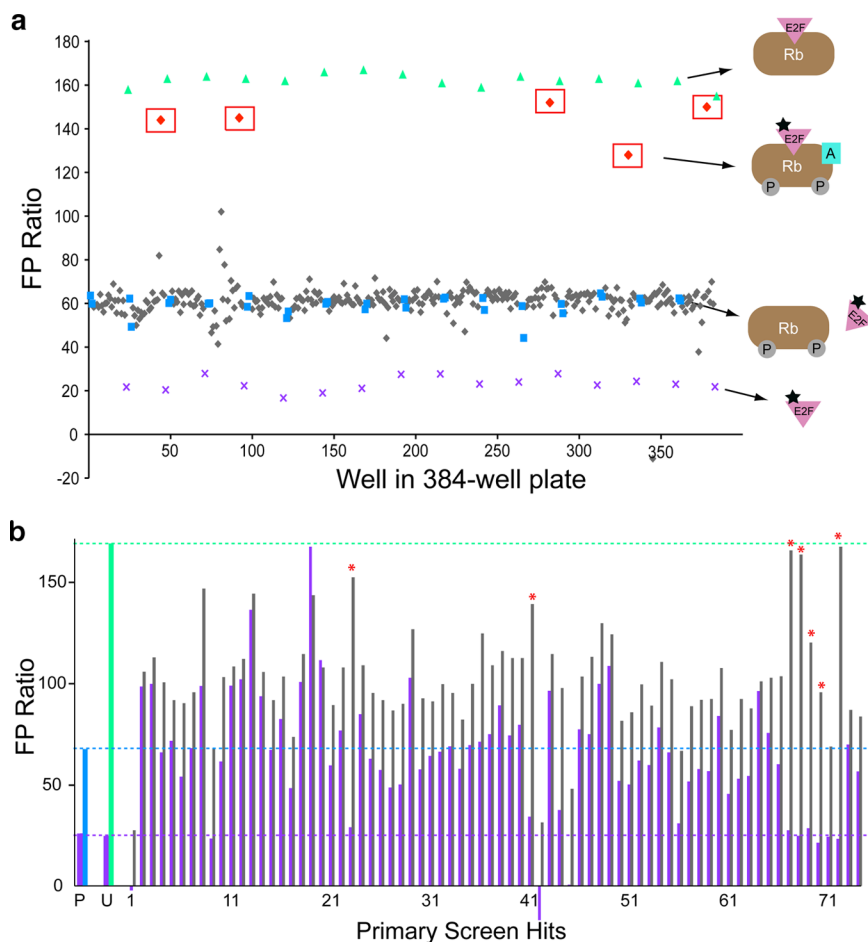


Figure 1. Fluorescence polarization screen for enhancers of Rb–E2F binding. (a) Sample data from the primary screen. FP ratio is plotted for each well in a 384-well plate. The wells contain phosphorylated Rb^{NP} and compounds (gray diamonds) or DMSO (blue squares, “negative control”), unphosphorylated Rb^{NP} (green triangles, “positive control”), or free E2F^{TMR} alone (purple crosses). The boxed red diamonds are hits that increase the FP ratio of E2F^{TMR} in the presence of phosphorylated Rb^{NP}. (b) Follow-up assay in which the effect of the compounds on E2F^{TMR} FP ratio was determined in the absence (purple bars) and presence (gray bars) of phosphorylated Rb^{NP}. The phosphorylated Rb^{NP} negative (P, blue bar) and unphosphorylated Rb^{NP} (U, green bar) positive controls are shown on the left. Hits were validated (red asterisks) if they yielded low FP ratios similar to controls in the Rb^{NP} target-minus (dashed purple line) assay and high FP ratios in the Rb^{NP} target-positive assay (dashed green line).

increases upon addition of 10 nM phosphorylated Rb^{NP} and 10 nM unphosphorylated Rb^{NP} to ~60 and ~165, respectively. The more modest FP ratio increase upon addition of phosphorylated Rb^{NP} reflects its approximately 10-fold weaker affinity for E2F^{TMR} compared to the affinity of unphosphorylated Rb^{NP} for E2F^{TMR}.¹⁴ We conducted a pilot screen using a 21 120 small molecule library from ChemDiv that contains groups of analogs based on ~1200 structurally diverse “drug-like” scaffolds. Fifty μ M of each compound was incubated with 20 nM phosphorylated Rb^{NP}, and then 10 nM E2F^{TMR} was added. Control wells were used that had no protein (E2F^{TMR}-only) or had 0.5% (by volume) DMSO added to either unphosphorylated or phosphorylated Rb^{NP}.

Sample data from one 384-well plate are shown in Figure 1a, and results for the entire screen can be seen in Supporting Figure S1. We looked for hit compounds that raised the FP ratio toward that of unphosphorylated, tighter-binding Rb^{NP}. In this primary screen, the assay had an average $Z' = 0.82 \pm 0.02$.¹⁸ 74 compounds were selected as hits (0.35% hit rate) that had FP ratios higher than the average FP of phosphorylated Rb^{NP} with B-scores¹⁹ of 10 (Z-score of 7.7) or higher. These hits also satisfied the criterion that the measured overall fluorescence intensity was less than three

standard deviations above average control fluorescence intensity.

We recognized that because we are seeking compounds that increase the FP ratio, which reflects enhanced Rb binding, a molecule that induces E2F^{TMR} aggregation would be detected in the screen as a hit.²⁰ To rule out these false-positives, we tested screen hits in a follow-up “target-minus” assay in which phosphorylated Rb^{NP} was left out (Figure 1b). Most of the initial hits resulted in a perturbed FP ratio in the absence of a target, likely the result of either intrinsic fluorescence or compound induced aggregation of the TMR-peptide. We did find seven hits in the library that induced no effect in the absence of Rb^{NP} and enhanced the FP ratio in the presence of phosphorylated Rb^{NP} (red asterisks in Figure 1b and Supporting Information Table). Four of the seven compounds increased the affinity of E2F^{TMR} for phosphorylated Rb^{NP} in a complete protein titration (Supporting Information Figure S2). Those four validated hits contain a common core scaffold based on 1,6-dimethylpyrimido[5,4-*e*][1,2,4]triazene-5,7(1H,6H)-dione. Such triazene compounds are known to generate reactive oxygen species (ROS) that may induce off-target effects in cells.²¹ We found that triazene compound activity in

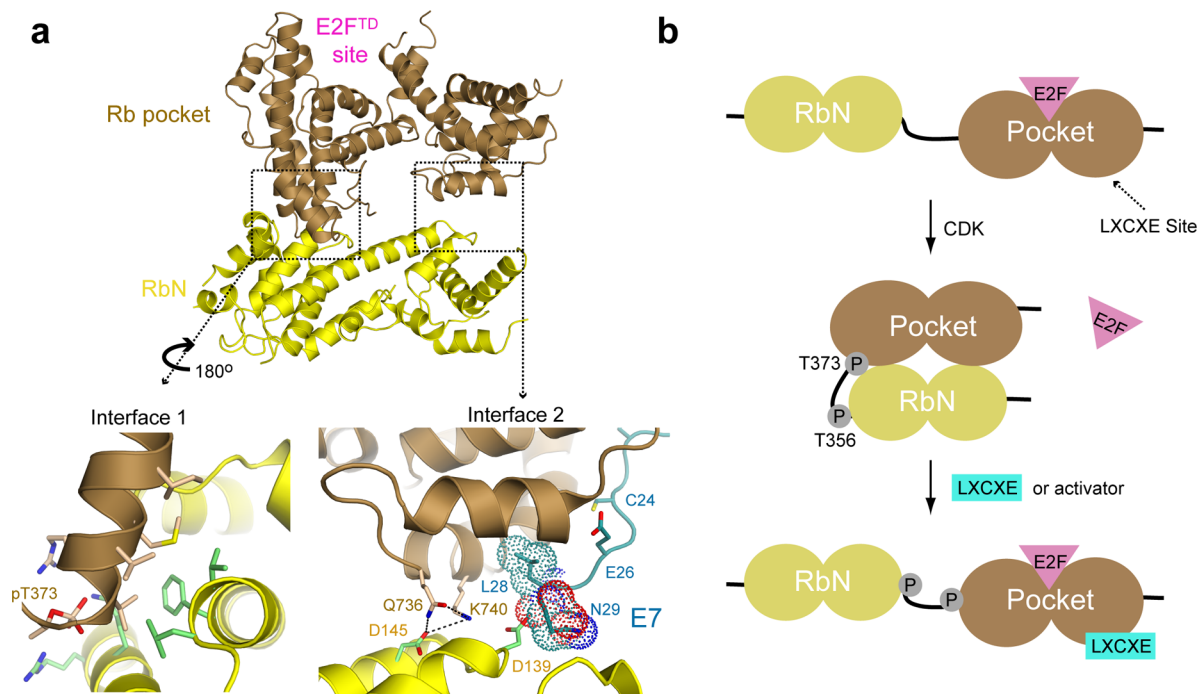


Figure 2. Structure-based strategy for activation of Rb. (a) Structure of phosphorylated Rb (from PDB code: 4ELJ). Docking between the Rb N-terminal domain (RbN, yellow) and the pocket domain (brown) occurs across two interfaces. Interface 1 is mediated by a pocket helix that is nucleated by Thr373 phosphorylation. Interface 2 is near the LxCxE-binding cleft in the pocket. The E7 peptide (cyan backbone), which is shown bound at its site in the unphosphorylated pocket (from PDB code: 1GUX), clashes with RbN residue Asp139 at the interface. (b) Phosphorylation of sites in the Rb interdomain linker induces a conformational change that allosterically inhibits E2F^{TD} binding. We find that an LxCxE peptide acts as an activator by binding Rb and inhibiting the RbN-pocket interdomain association.

the FP assay was lost in the presence of catalase (not shown), so we did not pursue them further.

We next explored a strategy for developing Rb activators that are motivated by the structural mechanism underlying how the Rb–E2F^{TD} complex is inhibited by Rb phosphorylation (Figure 2).¹⁴ Thr373 phosphorylation induces an interdomain association between RbN and the pocket, which allosterically opens the E2F^{TD} binding cleft to weaken affinity. RbN-pocket association occurs across two interfaces (Figure 2a), both of which must be formed to open up the E2F^{TD}-binding site and disrupt interactions between the pocket and E2F^{TD}. One interface is anchored by the first helix of the pocket domain, which is nucleated by Thr373 phosphorylation and docks into a hydrophobic groove in RbN. The RbN position at the second interface is close to the LxCxE binding site in the pocket domain (see for example the structure of the human papilloma virus (HPV) E7 LxCxE peptide-pocket domain complex).^{10,14} From a structural alignment (Figure 2a), the binding of the LxCxE peptide and interdomain docking appear incompatible.

We reasoned that molecules that inhibit interdomain docking would stabilize E2F^{TD} binding to phosphorylated Rb by preventing the allosteric opening of the E2F binding site (Figure 2b). Moreover, because the LxCxE peptide binds near the second RbN-pocket interface (interface 2 in Figure 2a), we hypothesized that the LxCxE peptide would disrupt docking and act as an activator. We tested the effects of the LxCxE peptide from the HPV E7 protein on E2F^{TMR} binding to Rb^{NP} using the FP assay as in the pilot screen but using a full protein titration (Figure 3a). The affinity of E2F^{TMR} for unphosphorylated Rb^{NP} ($K_d = 4.3 \pm 0.2$ nM) is 8-fold tighter than its affinity for phosphorylated Rb^{NP} ($K_d = 31 \pm 4$ nM). In the presence of 10 μ M E7 LxCxE peptide, phosphorylated Rb^{NP} binds E2F^{TMR}

with 2-fold higher affinity ($K_d = 16 \pm 2$ nM), which implicates the LxCxE peptide as an example of a desired Rb activator molecule. In the presence of 2 μ M full length E7 protein, E2F^{TMR} binds phosphorylated Rb^{NP} even tighter ($K_d = 4.6 \pm 0.3$ nM) and with similar affinity as unphosphorylated Rb^{NP}.

We found that the LxCxE peptide and full-length E7 increased Rb^{NP}–E2F^{TMR} affinity with $EC_{50} = 190 \pm 40$ nM and $EC_{50} = 10 \pm 2$ nM, respectively (Figure 3b). The greater potency of the full-length protein correlates with its known 20-fold greater affinity for the Rb pocket domain.²² We suggest that the greater highest activity of the E7 protein (~100%) compared to the LxCxE peptide (~70%) may result from the fact that its larger size is better suited for occluding the RbN-pocket interface. We found that the LxCxE-peptide and E7 protein do not affect E2F^{TD} binding to Rb if the docking interface is mutated (Q736A/K740A; Supporting Information Figure 3), which supports further our proposal that these activators function by disrupting interdomain docking. We also tested two LxCxE-like peptides from cyclin D (no hydrophobic in +2 position) and LINS2 (LxSxE), which have weak affinity for Rb.²³ These variant peptides and a compound previously reported to bind the LxCxE cleft (compound #478337 from Fera et al.⁹) show no effect in the Rb activation assay (Figure 3b).

To confirm the stabilizing effect of the LxCxE peptide in an orthogonal assay, we measured affinities using isothermal titration calorimetry (Figure 4). We found that E2F1^{TD} binds unphosphorylated Rb^{NP} with similar affinity in the absence ($K_d = 70 \pm 20$ nM) and presence ($K_d = 110 \pm 20$ nM) of excess E7 LxCxE peptide (Figure 4a). In contrast, the affinity of E2F1^{TD} for phosphorylated Rb^{NP} is enhanced in the presence of LxCxE peptide ($K_d = 340 \pm 20$ nM) compared to in its absence ($K_d =$

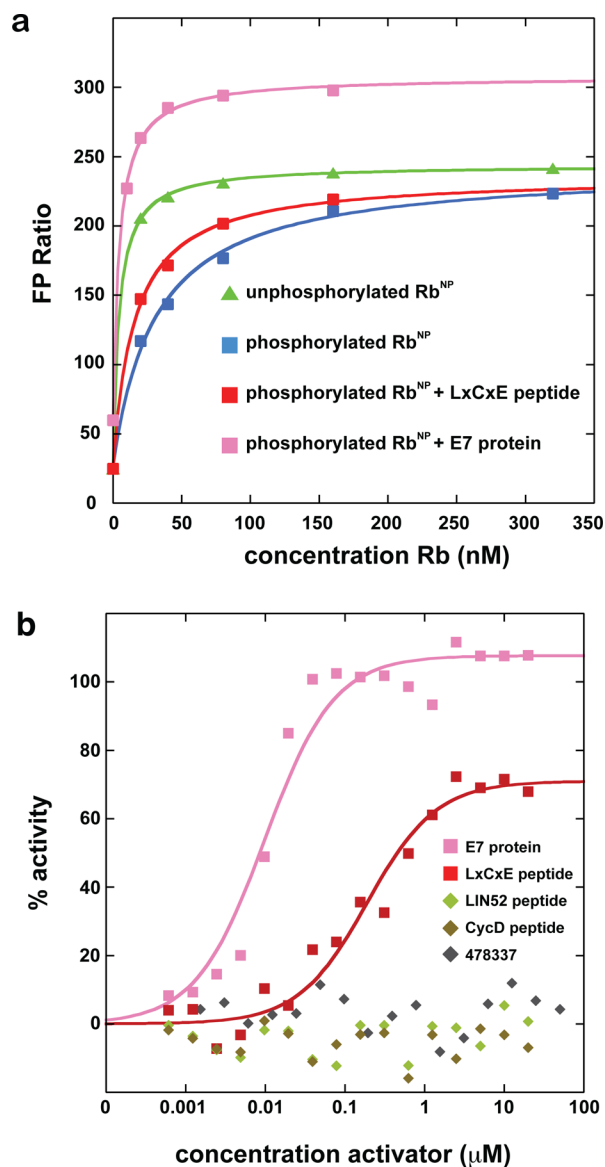


Figure 3. LxCxE peptide shown to act as an Rb activator. (a) Titration of unphosphorylated and phosphorylated Rb^{NP} into E2F^{TMR}. In the presence of the E7 LxCxE peptide and full-length E7 protein, the affinity is increased. (b) EC₅₀ measurements of LxCxE peptide and E7 protein activity. Compound #478337 from Fera *et al.*⁹ and LxCxE variant peptides from cyclin D and LIN52 do not show activity.

750 \pm 10 nM; Figure 4b). The observed increase in affinity that is specific for phosphorylated Rb demonstrates that molecules that interfere with the structural changes induced by Rb phosphorylation can act as Rb activators. We note that while the fold-change due to the LxCxE peptide is similar in the ITC assay as in the FP assay, measured Rb^{NP}–E2F affinities are greater using FP, perhaps due to the hydrophobic TMR dye.

In conclusion, we have developed a robust fluorescence polarization assay for screening molecules that modulate the binding between Rb and E2F, and we found that an LxCxE peptide from the HPV E7 protein, which is known to bind at the RbN-pocket interface,^{10,14} increases affinity of the complex. Several observations support the idea that isolated LxCxE peptides or derivatives could be used as Rb–E2F stabilizers in cells. While the E7 and related viral oncoproteins disrupt Rb–E2F complexes in cells to stimulate proliferation, in each case

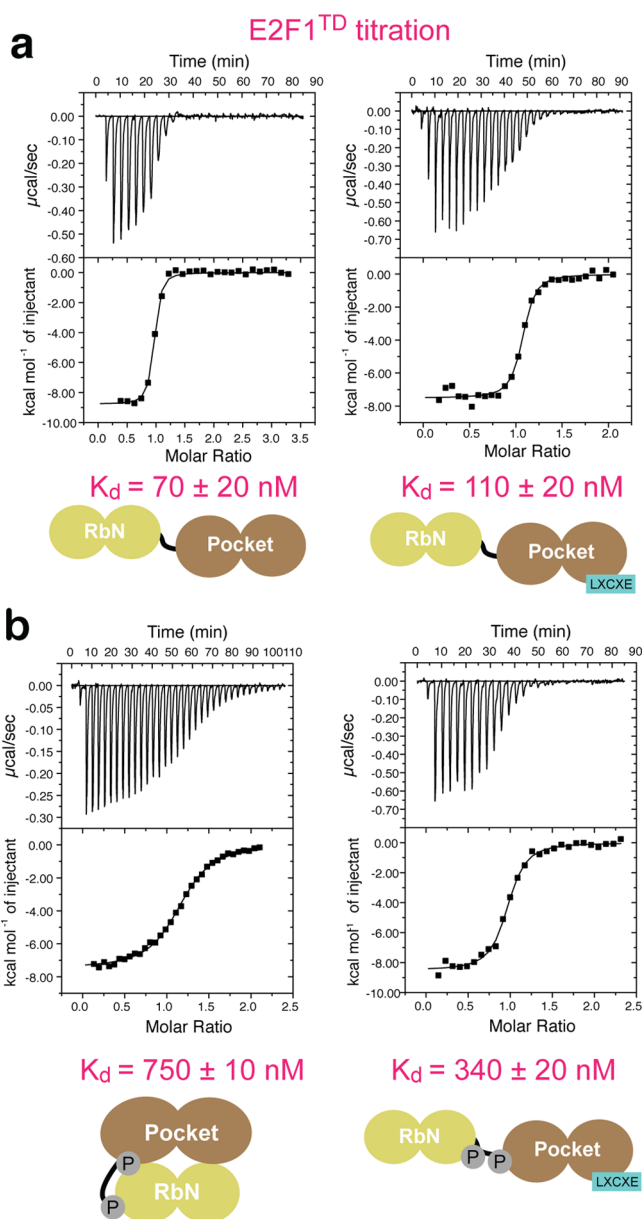


Figure 4. The E7 LxCxE peptide increases affinity of E2F^{TD} for phosphorylated Rb. Representative ITC curves and average K_d measurements are shown for E2F1^{TD} titration into unphosphorylated (a) and phosphorylated (b) Rb^{NP}.

the LxCxE-containing domain is insufficient. Additional domains that directly inhibit Rb–E2F association are required, and in the case of E7, the additional domain targets binding of the Rb C-terminal domain to E2F.^{24–26} Notably, expression of an SV40 virus T-antigen protein mutant, which contains the LxCxE motif but lacks the Rb–E2F dissociating domain, enhances the population of Rb–E2F complexes relative to free E2F in fibroblast cells.²⁶ Moreover, the fact that T373 mutation inhibits Rb–E2F dissociation and E2F activation in cells^{15–17} suggests that the affinity increase achieved here, which negates the effect of T373 phosphorylation, may effectively modulate Rb activity *in vivo*.

While the E7 LxCxE peptide is effective *in vitro*, its likely poor pharmacokinetic properties and extended binding structure make it a suboptimal lead for a therapeutic or chemical probe. However, we envision developing peptide

mimics that circumvent these shortcomings such as stapled or cyclic peptides. A group of thiadiazolidinedione compounds has been reported to competitively inhibit Rb-LxCxE association.⁹ In an experiment with one such compound reported to bind Rb with 200 nM affinity (#478337 in Fera et al.⁹), we did not observe any effect on E2F^{TD} affinity for phosphorylated Rb^{NP} (Figure 3b). It may be that the specific molecular requirements of inhibiting viral protein LxCxE binding to the pocket cleft and disrupting the RbN-pocket interdomain docking are distinct. Indeed, the location of the LxCxE peptide-binding site is adjacent to but not directly overlapping the interdomain interface (Figure 2a). The full-length E7 protein may be a more effective activator than the peptide (Figure 3) because additional interactions occlude this interface. We propose that LxCxE_{ExL} peptide derivatives may be more active if they are extended at their C-terminus to overlap more extensively with the RbN docking surface in the pocket. As seen in Figure 2a, N29 (in the +1 position relative to the second L in the LxCxE_{ExL} motif) clashes with RbN, and addition of optimized chemical groups at this end may impinge more on pocket–RbN interactions. With respect to further screening, our results suggest that libraries containing compounds with larger scaffolds, such as natural products derived libraries, may be more suitable for producing lead activators. We anticipate that ideal compounds would access the hydrophobic pocket bound by the second leucine in the “LxCxE_{ExL}” peptide and also contact the Gln736/Lys740 surface that forms the docking interface (Figure 2a).

In addition to the molecules discussed here, we propose developing Rb activators that bind the RbN groove forming the primary RbN-pocket interface (interface 1 in Figure 2a). By inhibiting docking of the phosphorylated pocket helix, these molecules may stabilize E2F^{TD} binding to phosphorylated Rb as desired. The pocket helix contacts the groove using hydrophobic residues along one face of an amphipathic helix. This type of interaction has been successfully targeted by small molecules.^{27–30} A classic example is the p53–MDM2 interface, formed by residues in the *i*, *i* + 4, and *i* + 7 positions of a p53 helix, for which *cis*-imidazole (Nutlin) and spiro-oxindole (MI-219) inhibitors have been found.^{29,30} Therefore, while our screen results suggest that disrupting the RbN-pocket association is a challenge for small molecules, recent successes in protein–protein interaction inhibition suggest the promise of finding a lead compound for direct Rb activation.

METHODS

Protein and Peptide Reagents. Rb^{NP} and E2F1^{TD} (E2F1 residues 409–426) were expressed in *E. coli* as GST-fusion proteins and purified with GS4B sepharose as previously described.¹⁴ Following elution from the affinity resin, the fusion protein was diluted 3-fold into a buffer containing 25 mM Tris and 1 mM DTT (pH 8.0). Protein was then loaded onto a Source Q ion exchange column equilibrated in the same low salt buffer and eluted from the column in a gradient of 0–1 M NaCl. The fusion protein eluted in a single peak and was digested overnight at 4 °C in the presence of 1% (by mass) TEV protease. The samples were loaded again onto GS4B to remove the free GST, and the proteins were collected and concentrated to ~5 mg mL⁻¹ for future assays. Phosphorylation of Rb^{NP} was achieved as previously described using 10% (by mass) purified Cdk2–CycA in a reaction containing 5 mM ATP and 20 mM MgCl₂.¹³ After an overnight reaction at 4 °C, quantitative phosphorylation on two sites was validated by observation of an increase in molecular mass of ~160 Da using electrospray ionization mass spectrometry (Supporting Information Figure 4). Synthetic E7 LxCxE (DLYCYEQLN), LIN52 (TDLEASLLSFEKLDRAphosSPDLWPE), cyclin D (MEHQLLCC-

VETIRRAY), and TMR-E2F2^{TD} (QDDYLWGLEAGEGIDSLFD) peptides were ordered from Genscript, LLC.

Isothermal Titration Calorimetry. ITC experiments were performed with a VP-ITC calorimeter from Microcal, LLC (now supported by Malvern Instruments). Prior to the measurements, unphosphorylated and phosphorylated Rb^{NP} and E2F1^{TD} were dialyzed overnight in the same beaker against a buffer containing 40 mM Tris, 100 mM NaCl, and 1 mM 2-mercaptoethanol (pH 8.0). Measurements were made with an E2F1^{TD} concentration of 1 mM, an Rb^{NP} concentration of 15–25 μM, and an LxCxE peptide concentration of 100 μM. The reported *K*_d values are the average of 2–3 measurements, and the standard deviation is reported as the error.

Fluorescence Polarization Assay and Screen. Fluorescence polarization measurements were made in black, untreated 384-well plates (Corning). For the screen, 20 μL of a 40 nM solution of Rb^{NP} was dispensed using a Matrix Wellmate peristaltic pump. Compounds or DMSO were pin-transferred using a 200 nL pin tool (PerkinElmer) to a final concentration of 50 μM. Then, 20 μL of a 20 nM E2F^{TMR} solution was added for a resulting final concentration of 20 nM Rb^{NP} and 10 nM E2F^{TMR}. All solutions were prepared using a buffer containing 40 mM Tris, 100 mM NaCl, 1 mM DTT, and 0.1% Tween-20 (pH 8.0). Total fluorescence and fluorescence polarization were measured using a PerkinElmer Envision plate reader. An excitation filter centered around a wavelength of 531 nm and with a bandwidth of 20 nm was used along with an emission filter centered around 595 nm and with a bandwidth of 60 nm. Fluorescence polarization ratios were calculated as $FP = 1000(S - G \times P)/(S + G \times P)$, where *S* is intensity of fluorescence parallel to excitation plane, *P* is perpendicular fluorescence intensity, and *G* is a correction factor to ensure positive ratio values. For the protein titration experiments, 10 μM of E7 LxCxE peptide, 2 μM of E7 protein, or 50 μM compound was added to prepared solutions of Rb^{NP} at the different indicated concentrations. Binding constants were determined from fits of the protein titration data using a two-site binding model, and the *y* intercept was fixed to the FP value of the E2F^{TMR} peptide alone. Reported errors in the *K*_d from FP measurements are curve-fitting errors. The EC50 measurement was performed using conditions similar to the screen except 20 nM Rb^{NP} was used. We report % activity = $(FP_{\text{phosRb+activator}} - FP_{\text{phosRb}})/(FP_{\text{unphosRb}} - FP_{\text{phosRb}})$.

ASSOCIATED CONTENT

Supporting Information

The Supporting Information is available free of charge on the ACS Publications website at DOI: 10.1021/acschembio.6b00011.

Supporting Figures 1–4, Supporting Table 1 (PDF)

AUTHOR INFORMATION

Corresponding Author

*E-mail: srubin@ucsc.edu.

Notes

The authors declare no competing financial interest.

ACKNOWLEDGMENTS

This work was supported by the U.S. Army Medical Research and Materiel Command, through the Breast Cancer Research Program under Award No. W81XWH-14-1-0329 to S.M.R. Opinions, interpretations, conclusions, and recommendations are those of the author and are not necessarily endorsed by the U.S. Army. This work was also supported by grant R01CA132685 from the National Cancer Institute to S.M.R. and by the Santa Cruz Cancer Benefit Group. The high-throughput screening performed in the UCSC Chemical Screening Center was supported by NIH shared instrumentation grant 1 S10 RR022455.

REFERENCES

- (1) Burkhart, D. L., and Sage, J. (2008) Cellular mechanisms of tumour suppression by the retinoblastoma gene. *Nat. Rev. Cancer* 8, 671–682.
- (2) Classon, M., and Harlow, E. (2002) The retinoblastoma tumour suppressor in development and cancer. *Nat. Rev. Cancer* 2, 910–917.
- (3) Dick, F. A., and Rubin, S. M. (2013) Molecular mechanisms underlying RB protein function. *Nat. Rev. Mol. Cell Biol.* 14, 297–306.
- (4) Lipinski, M. M., and Jacks, T. (2000) The retinoblastoma gene family in differentiation and development. *Oncogene* 18, 7873–7882.
- (5) Knudsen, E. S., and Knudsen, K. E. (2008) Tailoring to RB: tumour suppressor status and therapeutic response. *Nat. Rev. Cancer* 8, 714–724.
- (6) Malumbres, M., and Barbacid, M. (2001) To cycle or not to cycle: a critical decision in cancer. *Nat. Rev. Cancer* 1, 222–231.
- (7) Sherr, C. J. (1996) Cancer cell cycles. *Science* 274, 1672–1677.
- (8) Stone, A., Sutherland, R. L., and Musgrove, E. A. (2012) Inhibitors of cell cycle kinases: recent advances and future prospects as cancer therapeutics. *Crit. Rev. Oncog.* 17, 175–198.
- (9) Fera, D., Schultz, D. C., Hodawadekar, S., Reichman, M., Donover, P. S., Melvin, J., Troutman, S., Kissil, J. L., Huryn, D. M., and Marmorstein, R. (2012) Identification and characterization of small molecule antagonists of pRb inactivation by viral oncoproteins. *Chem. Biol.* 19, 518–528.
- (10) Lee, J. O., Russo, A. A., and Pavletich, N. P. (1998) Structure of the retinoblastoma tumour-suppressor pocket domain bound to a peptide from HPV E7. *Nature* 391, 859–865.
- (11) Rubin, S. M. (2013) Deciphering the retinoblastoma protein phosphorylation code. *Trends Biochem. Sci.* 38, 12–19.
- (12) Lees, J. A., Buchkovich, K. J., Marshak, D. R., Anderson, C. W., and Harlow, E. (1991) The retinoblastoma protein is phosphorylated on multiple sites by human cdc2. *EMBO J.* 10, 4279–4290.
- (13) Burke, J. R., Deshong, A. J., Pelton, J. G., and Rubin, S. M. (2010) Phosphorylation-induced conformational changes in the retinoblastoma protein inhibit E2F transactivation domain binding. *J. Biol. Chem.* 285, 16286–16293.
- (14) Burke, J. R., Hura, G. L., and Rubin, S. M. (2012) Structures of inactive retinoblastoma protein reveal multiple mechanisms for cell cycle control. *Genes Dev.* 26, 1156–1166.
- (15) Brown, V. D., Phillips, R. A., and Gallie, B. L. (1999) Cumulative effect of phosphorylation of pRB on regulation of E2F activity. *Mol. Cell Biol.* 19, 3246–3256.
- (16) Knudsen, E. S., and Wang, J. Y. (1997) Dual mechanisms for the inhibition of E2F binding to RB by cyclin-dependent kinase-mediated RB phosphorylation. *Mol. Cell Biol.* 17, 5771–5783.
- (17) Lents, N. H., Gorges, L. L., and Baldassare, J. J. (2006) Reverse mutational analysis reveals threonine-373 as a potentially sufficient phosphorylation site for inactivation of the retinoblastoma tumor suppressor protein (pRB). *Cell Cycle* 5, 1699–1707.
- (18) Zhang, J. H., Chung, T. D., and Oldenburg, K. R. (1999) A Simple Statistical Parameter for Use in Evaluation and Validation of High Throughput Screening Assays. *J. Biomol. Screening* 4, 67–73.
- (19) Brideau, C., Gunter, B., Pikounis, B., and Liaw, A. (2003) Improved statistical methods for hit selection in high-throughput screening. *J. Biomol. Screening* 8, 634–647.
- (20) Irwin, J. J., Duan, D., Torosyan, H., Doak, A. K., Ziebart, K. T., Sterling, T., Tumanian, G., and Shoichet, B. K. (2015) An Aggregation Advisor for Ligand Discovery. *J. Med. Chem.* 58, 7076–7087.
- (21) Johnston, P. A. (2011) Redox cycling compounds generate H₂O₂ in HTS buffers containing strong reducing reagents—real hits or promiscuous artifacts? *Curr. Opin. Chem. Biol.* 15, 174–182.
- (22) Jones, R. E., Wegryz, R. J., Patrick, D. R., Balishin, N. L., Vuocolo, G. A., Riemen, M. W., Defeo-Jones, D., Garsky, V. M., Heimbrook, D. C., and Oliff, A. (1990) Identification of HPV-16 E7 peptides that are potent antagonists of E7 binding to the retinoblastoma suppressor protein. *J. Biol. Chem.* 265, 12782–12785.
- (23) Guiley, K. Z., Liban, T. J., Felthousen, J. G., Ramanan, P., Litovchick, L., and Rubin, S. M. (2015) Structural mechanisms of DREAM complex assembly and regulation. *Genes Dev.* 29, 961–974.
- (24) Fattaey, A. R., Harlow, E., and Helin, K. (1993) Independent regions of adenovirus E1A are required for binding to and dissociation of E2F-protein complexes. *Mol. Cell Biol.* 13, 7267–7277.
- (25) Patrick, D. R., Oliff, A., and Heimbrook, D. C. (1994) Identification of a novel retinoblastoma gene product binding site on human papillomavirus type 16 E7 protein. *J. Biol. Chem.* 269, 6842–6850.
- (26) Zalvide, J., Stubdal, H., and DeCaprio, J. A. (1998) The J domain of simian virus 40 large T antigen is required to functionally inactivate RB family proteins. *Mol. Cell Biol.* 18, 1408–1415.
- (27) Bullock, B. N., Jochim, A. L., and Arora, P. S. (2011) Assessing helical protein interfaces for inhibitor design. *J. Am. Chem. Soc.* 133, 14220–14223.
- (28) Cummings, C. G., and Hamilton, A. D. (2010) Disrupting protein-protein interactions with non-peptidic, small molecule alpha-helix mimetics. *Curr. Opin. Chem. Biol.* 14, 341–346.
- (29) Grasberger, B. L., Lu, T., Schubert, C., Parks, D. J., Carver, T. E., Koblisch, H. K., Cummings, M. D., LaFrance, L. V., Milkiewicz, K. L., Calvo, R. R., Maguire, D., Lattanze, J., Franks, C. F., Zhao, S., Ramachandren, K., Bylebyl, G. R., Zhang, M., Manthey, C. L., Petrella, E. C., Pantoliano, M. W., Deckman, I. C., Spurlino, J. C., Maroney, A. C., Tomczuk, B. E., Molloy, C. J., and Bone, R. F. (2005) Discovery and cocrystal structure of benzodiazepinedione HDM2 antagonists that activate p53 in cells. *J. Med. Chem.* 48, 909–912.
- (30) Vassilev, L. T., Vu, B. T., Graves, B., Carvajal, D., Podlaski, F., Filipovic, Z., Kong, N., Kammlott, U., Lukacs, C., Klein, C., Fotouhi, N., and Liu, E. A. (2004) In vivo activation of the p53 pathway by small-molecule antagonists of MDM2. *Science* 303, 844–848.